Supporting Information

belonging to

The pH Induced Sol-Gel Transition in Skim Milk Revisited – A Detailed Study Using Time-Resolved Light- and X-Ray Scattering Experiments

Christian Moitzi, Andreas Menzel, Peter Schurtenberger , and Anna Stradner

A. Theoretical calculation of the structure factor effect on casein micelles.

The theoretical calculation of the structure factor $S(q)$ in colloidal suspensions requires the assumption of a model for the interaction potential. A simple and often realistic model potential for colloidal suspensions is the hard sphere potential. The resulting structural properties of a hard sphere suspension are characterized by only two parameters, the particle radius and the volume fraction. By applying the Percus-Yevick closure relation in the Ornstein-Zernike equation, one can calculate the scattered intensity as a function of the scattering vector for a mixture of particles. This can be done in a closed form, so that the structure factor can be calculated exactly for all types of size distributions.

The size distribution of casein micelles was measured independently with various methods. It is very broad, ranging from 30 nm to 300 nm in radius. The maximum of the size distribution is located at about 100 nm, but the distribution exhibits a weak tail to large radii. We were using a Schultz-Zimm distribution to fit the experimental result (Figure S1a). This distribution was then used to calculate the structure factor as a function of the volume fraction of particles assuming hard sphere interactions (Figure S1b). These theoretical structure factors were then multiplied with the form factor of casein micelles measured at high dilution and compared with the experimental values which were determined at the casein concentration which approximately corresponds to this volume fraction (Figure S1c). There is a good agreement between the theory and the experimental results up to the natural concentration of casein in milk (volume fraction about 0.1). The only major difference is an apparent shift in the absolute values at the highest concentration. This is most probably due to an error in the transmission measurement required to properly normalize the data obtained with the 3DDLS instrument. This results in a systematic shift of the intensities, while the shape of the scattering curve is not affected. Due to the extremely high turbidity of skim milk at its natural concentration an accurate measurement of the transmission, excluding the light which is scattered into forward direction, is not easy. Considering the experimental difficulties associated with the measurement of the absolute singly scattered intensity in a sample as turbid as undiluted skim milk (transmission as low as 0.01 in a cell with a path length of 1.6 mm), the deviations of the result from the theory are surprisingly small. The results show that we can measure and quantitatively calculate the structure facture effect of casein micelles in perfect analogy to model colloids.

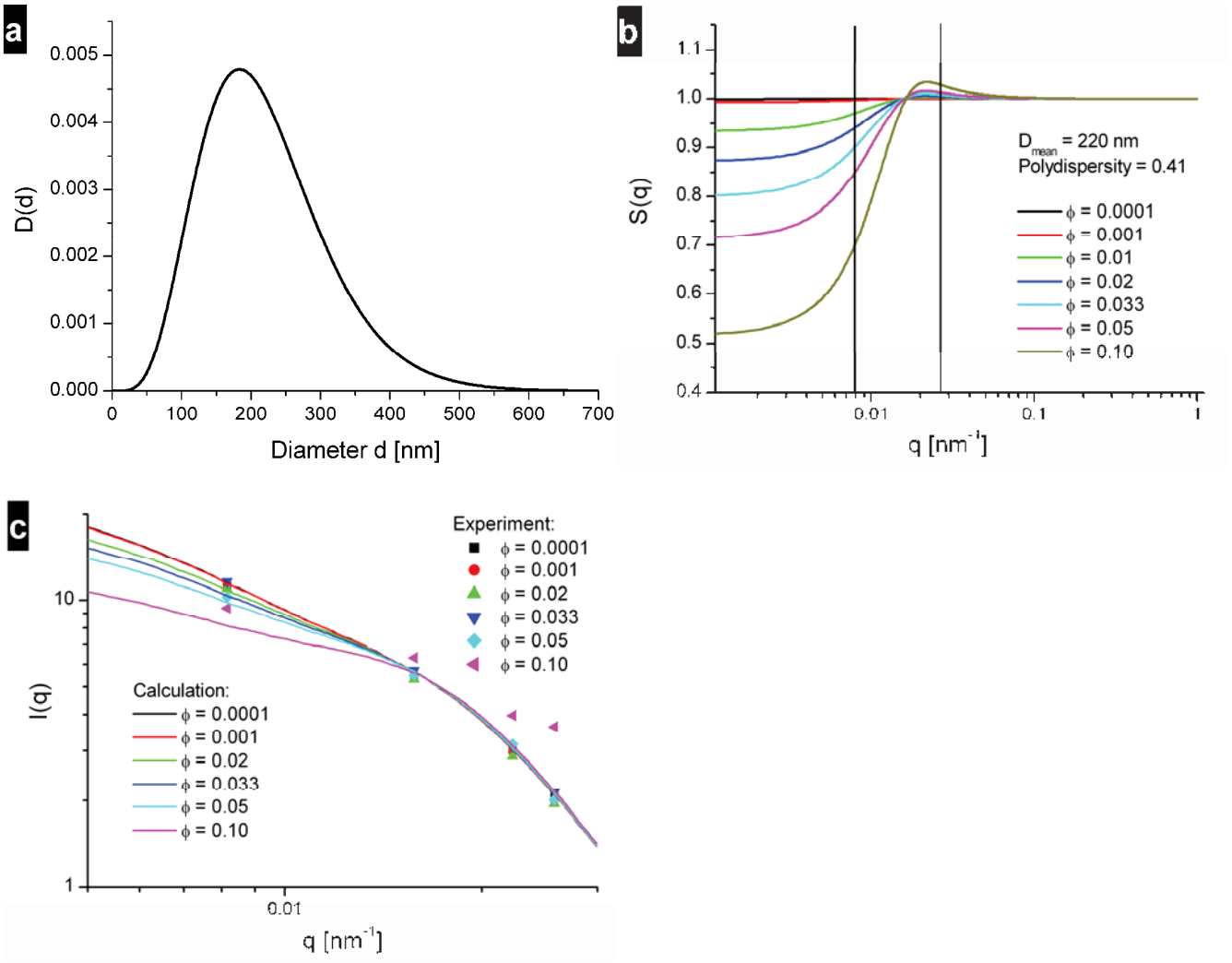

Figure S1. a. Approximated size distribution of casein micelles using a Schultz-Zimm function. The distribution is in agreement with literature results and our own results (see Figure S2). **b.** Polydisperse structure factor calculated from the size distribution shown in Figure S1a for various volume fractions. Hard sphere interaction was assumed. The vertical lines mark the *q*-range which is accessible with our light scattering instrument. **c.** Comparison of theory and experimental result. The theoretical structure factors from Figure S1b were multiplied with the form factor of casein micelles measured at high dilution (solid lines). The symbols correspond to obtained values at different concentrations using our multiangle 3DDLS instrument. The volume fractions were calculated based on a swelling ratio of about 3.

B. Evaluation of micellar size distribution as function of pH.

We have not only investigated the evolution of the average size and the radius of gyration, but also determined the size distribution as a function of pH (Figure S2). Here we have used a multi-angle Laplace inversion method developed previously in our group [1]. The size distribution found at neutral pH is in very good agreement with the ones determined by different methods in literature (electron micrographs, small-angle neutron scattering, dynamic light scattering) [2, 3]. One finds a main peak at about 100 nm and a tail up to a few hundred nanometers in radius. With decreasing pH the main peak shifts down to smaller values. At a pH value of 5.09 the maximum in the distribution is at approx. 70 nm. At even lower pH the trend changes. At pH 5.04 the main peak shifts back to larger sizes. At pH 4.99 the main peak is again at about 100 nm, but one already finds very large particles because of the onset of aggregation. During the whole process prior to aggregation, no significant change in the large particle fractions at 200 – 300 nm was found.

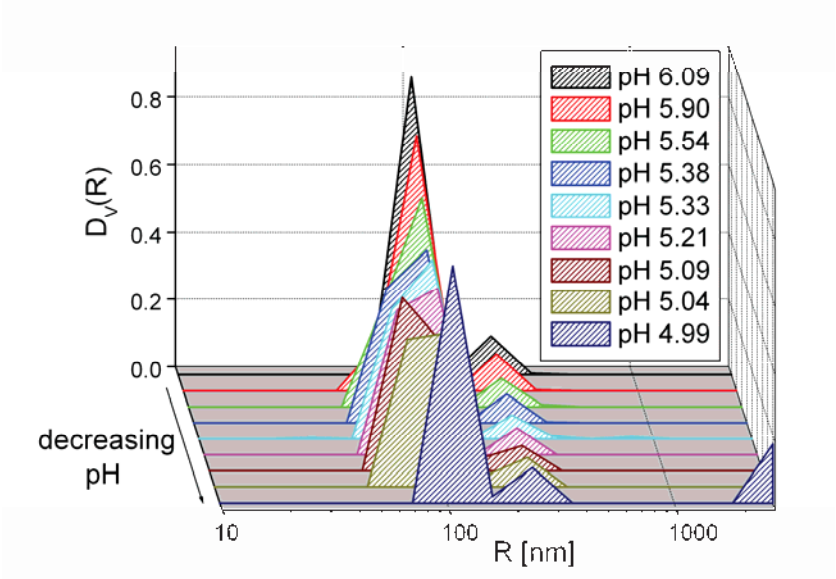

Figure S2. Particle size distribution functions of casein micelles for varying pH values (dilution (1+99)).

C. Internal mass distribution by small-angle x-ray scattering.

The information that can be obtained from light scattering is limited to overall quantities such as M, R_G and R_H due to the accessible q-range. The situation is quite different for SAXS, where larger q-values, corresponding to smaller distances in real space, are probed. Small-angle x-ray scattering can thus be used to determine the internal structure of the casein micelles. Because of the large photon flux at a modern synchrotron source one gets very good statistics after a measurement time of only 1 minute or even less. To avoid the problem of radiation damage due to the high x-ray intensity the sample cell was slightly shifted after every image taken with an exposure time of 1 s. Therefore it is easily possible to follow the acidification process in a time resolved way. In Figure S3a a few scattering curves of skim milk at various pH values are shown. One can clearly see changes in the local internal structure of the micelles which are reflected in the high q-regime. The information about the size and structure of the whole micelles is contained in the small q-regime. It has to be noted here that a detailed analysis of the internal structure of the micelles is difficult due to their large polydispersity in size and composition.

In Figure S3b the normalized forward scattering intensity $I(0)$ and radius of gyration R_G as function of the pH are shown. The overlap with the forward scattering intensity determined by light scattering experiments is very good (open symbols in Figure S3b). R_G is not changing significantly until the aggregation sets in. This is in perfect agreement with the results from light scattering as well.

In contrast to the light scattering experiments, where the physical size is accessible in terms of R_H, no comparable quantity is directly available from the SAXS data. However, Indirect Fourier Transformation (IFT) [4-8] gives access to the pair distance distribution function (PDDF), the extrapolation of the scattering intensities to a scattering angle of 0 ($I(0)$), and the radius of gyration (R_G). Furthermore, the convolution square root [9, 10] of the PDDF provides a determination of the radial distribution of the

excess scattering length density $\Delta\rho(r)$ assuming spherical geometry. In the case of x-ray scattering the radial contrast profile $\Delta\rho(r)$ is given by the electron density difference to water going from the center towards the surface of the micelle. Thus the IFT procedure followed by the convolution square root provides information not only about the size of the particles but also about their internal density profile. No details about this well established evaluation procedure are given here. Similar data treatment can be found in the literature [10-13].

To make the radial contrast profile easily comparable with the light scattering results (parameter R_G/R_H) a very simple model for the calculation was used. A profile of 3 steps, where the height and the position of the steps were varied to give the best fit to the experimental scattering curve, was assumed. It has to be noted that this assumption does not imply that the casein micelles are core-shell particles in reality. This model is certainly very much simplified, but it allows visualizing trends. The calculation resulted in a rather dense core and a rather loose shell in neutral milk (pH 6.17, Figure S3c). When the pH is shifted to lower values the core becomes less dense and eventually, when a pH of about 5 is reached, one gets an almost constant contrast profile. In the light scattering experiments the changes of the internal mass distribution were expressed in terms of the parameter R_G/R_H. There we found a low value of 0.6 at neutral pH (mass is concentrated in the center) and a value close to 0.775 at pH 5 (homogeneous particles).

In summary the results from x-ray scattering experiments are in perfect agreement with the light scattering. The fact that different types of radiation, different q-regimes, and a completely different type of data analysis were used for both methods gives strong support for the validity of the results.

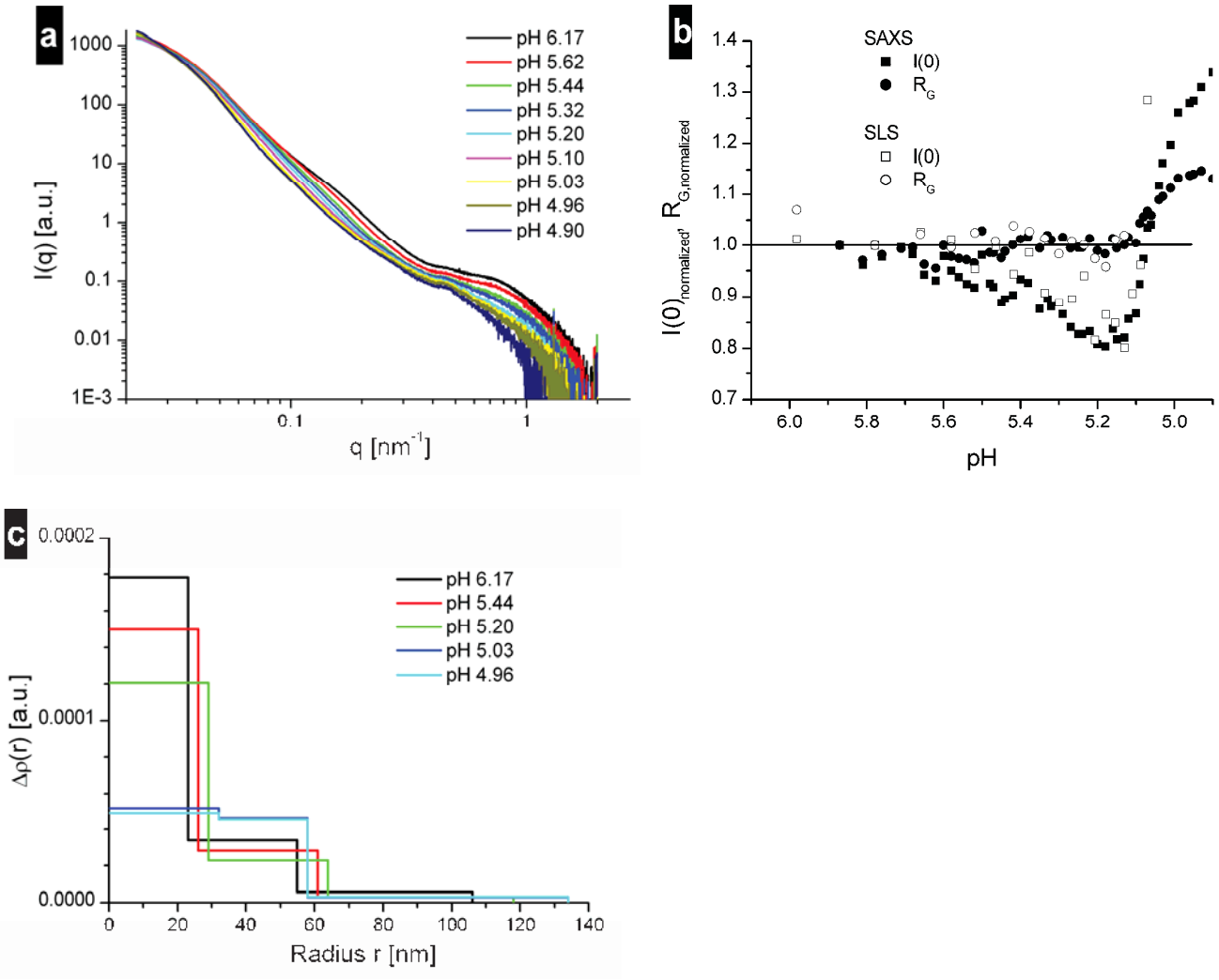

Figure S3. a. Small-angle x-ray scattering curves of undiluted skim milk at various pH values during acidification. **b.** Forward scattering intensity $I(0)$ and radius of gyration R_G as function of pH determined via indirect Fourier transformation of the curves shown in Figure S3a. $I(0)$ and R_G determined from light scattering experiments are shown for comparison (open symbols). **c.** Radial density distribution $\Delta\rho(r)$ for different pH values determined via indirect Fourier transformation followed by deconvolution. For the convolution square root spherical geometry was assumed.

D. References

1. Scheffold, F.; Shalkevich, A.; Vavrin, R.; Crassous, J.; Schurtenberger, P., *ACS Symposium Series* **2004,** *881*, 3-32.

2. Holt, C., *Advances in Protein Chemistry* **1992,** *43*, 63-151.

3. de Kruif, C. G., *J. Dairy Sci.* **1998,** *81*, 3019-3028.

4. Glatter, O., *J. Appl. Crystallogr.* **1977,** *10*, 415-421.

5. Glatter, O., *J. Appl. Crystallogr.* **1979,** *12*, 166-175.

6. Glatter, O.; Kratky, O., *Small angle X-ray scattering*. Academic Press: London, 1982; p 515.

7. Bergmann, A.; Fritz, G.; Glatter, O., *J. Appl. Crystallogr.* **2000,** *33*, 1212-1216.

8. Mittelbach, R.; Glatter, O., *J. Appl. Crystallogr.* **1998,** *31*, 600-608.

9. Glatter, O., *J. Appl. Crystallogr.* **1981,** *14*, 101-108.

10. Iampietro, D. J.; Brasher, L. L.; Kaler, E. W.; Stradner, A.; Glatter, O., *J. Phys. Chem. B* **1998,** *102*, 3105-3113.

11. Stubenrauch, K.; Moitzi, C.; Fritz, G.; Glatter, O.; Trimmel, G.; Stelzer, F., *Macromolecules* **2006,** *39* (17), 5865-5874.

12. Pedersen, J. S.; Schurtenberger, P., *J. Appl. Crystallogr.* **1996,** *29*, 646-661.

13. Schurtenberger, P.; Jerke, G.; Cavaco, C.; Pedersen, J. S., *Langmuir* **1996,** *12* (10), 2433-2440.